Phase Field Crystal Simulation during Plastic Deformation of Nanopolycrystal Metal

T. Hirouchi[1]*, T. Takaki[2], Y. Tomita[1]

[1] *Graduate School of Engineering, Kobe University, 1-1, Rokkodai, Nada, Kobe, 657-8501, Japan*
[2] *Graduate School of Science and Technology, Kyoto Institue of Technology, Matsugasaki, Sakyo, Kyoto, 606-8585, Japan*
e-mail: hirouchi@solid.mech.kobe-u.ac.jp, takaki@mech.kit.ac.jp, tomita@mech.kobe-u.ac.jp

Abstract
The optimum grain size, which is the transition point from grain-size hardening to grain-size softening in nanocrystalline metals, is determined using molecular dynamics (MD) simulation. However, the strain rate is unrealistically high since the time scale in MD is limited. Therefore, there is no confirmation whether the results in MD simulation under such a high strain rate can express deformation under a realistic strain rate. In this study, we studied the plastic deformation behavior of nanopolycrystalline materials under a low strain rate of about 10^0 s^{-1} by the phase field crystal method, which enables the expression of the local-time-averaged atomic behavior on diffusive time scales in a physical system. Additionally, the initial polycrystalline structure used in deformation simulation is generated during computational solidification. As a result of deformation simulation, it is confirmed that the mechanism underlying the deformation of nanopolycrystalline structures is intergranular deformation, such as grain rotation, grain coalescence or grain boundary migration driven by their curvature.

Key words: Phase Field Crystal Method, Multi-Scale Model, Nanopolycrystalline Metal, Plastic Deformation, Dislocation

INTRODUCTION

Industrial metallic materials usually contain many defects in microstructures that strongly affect their physical and chemical properties on the macroscopic scale. To improve the material properties and/or develop novel functions of such materials, it is essential to construct a computational model for predicting macroscopic properties that depend on microstructures. Although there are many computational strategies for investigating material properties, molecular dynamics (MD) and finite element (FE) simulations are widely used. Although MD simulations can compute the motions of individual molecules, their computational domain and time are restricted to a very small space (~10^9 atoms) and a very short time scale (~10^{-8} seconds), respectively. On the other hand, the FE method can treat arbitrary space and time scales. However, it is difficult to reproduce phenomena resulting from atomic structures, such as the grain size effects, using this method.

Recently, Elder *et al.* [1, 2] have proposed the phase field crystal (PFC) method. This method introduces a periodic order parameter that represents a local-time-averaged atomic density field to express regularly arranged atoms in solid crystals. In their papers [1-3], the periodic system's feature of naturally containing elastic effects is emphasized, and plastic deformation due to the generation, annihilation and motion of dislocations is represented spontaneously. Although these are also included in MD simulation, the PFC

method can describe systems on a diffusive time scale, which is much larger than that of atomic vibration. Therefore, it is suggested that PFC simulation can deal with a system having diffusive times and interatomic length scales. In this sense, the PFC method is anticipated as a model that bridges between a molecular description and a continuum field theory, or a multi-scale model.

The mechanical behavior of metallic materials depending on grain size is the most interesting point in material science and material industry. This typical relationship is known as the Hall-Petch (HP) relation, in which yield stress and the degree of work hardening monotonically increase with decreasing grain size. Recently, some experimental [5] and numerical [6, 7] studies have shown that the optimum grain size with the maximum strength, or the transition from a HP relation to an inverse HP relation, exists. It was clarified by MD simulations that intragranular and intergranular deformations are the predominant deformation modes in the regions of HP and inverse HP relations, respectively. However, the calculated flow stresses are obtained at a very high strain rate as compared with those obtained by experiments. The deformation mechanism and optimum grain size may change if simulations are performed at the same strain rate as that used in the experiment. The PFC method is believed to be feasible for simulating deformation behavior at a realistic strain rate.

In this study, by employing the PFC method, the deformation behavior of nanopolycrystalline structures with regular hexagonal grains is studied at a very low strain rate (about 10^0 s^{-1}). First, solidification is simulated to prepare regular grain structures with predetermined orientations. Next, the prepared structures are expanded by applying tension and the corresponding deformation behavior is investigated in detail.

PHASE FIELD CRYSTAL MODEL

Unlike the conventional phase field (PF) method, the phase field crystal (PFC) method [1, 2] uses an order parameter with a periodic profile in the state of free-energy minimization. This order parameter, or the phase field ϕ, is defined as a local-time-averaged atomic density on a time scale much larger than the vibrational period of atoms on the order of 10^{-15}s and smaller than diffusive time scales in a physical system. Therefore, the phase field is a conserved value. Figure 1 schematically shows the phase field profile around the solid-liquid interface one-dimensionally.
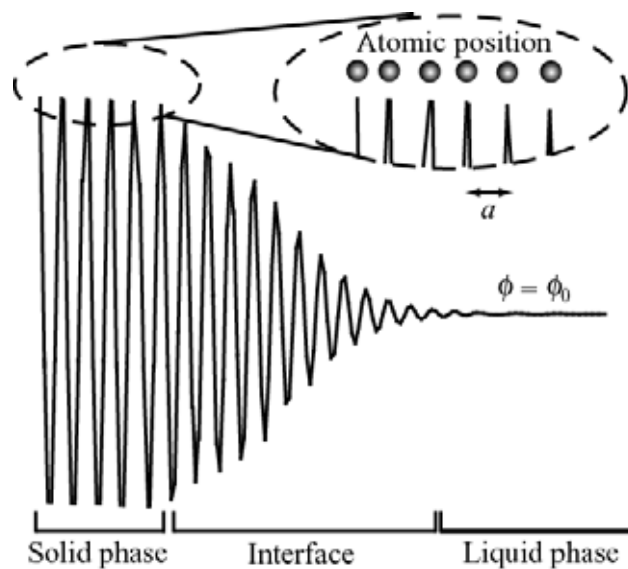

Fig. 1 Phase field profiles in PFC model.

In the steady solid phase of a material, atoms are perfectly fixed in a periodic arrangement. To express this condition, the phase field ϕ in the PFC method has a periodic profile with a wavelength a. The local maxima of the phase field ϕ correspond to the atomic positions shown in Fig. 1. Although, in the liquid phase of a real material, atomic position depends on time, the time-averaged atomic density at a point becomes constant. Therefore, the phase field ϕ is maintained constant inside a liquid phase. At the solid-liquid interface, the phase field changes smoothly from periodicity to a constant.

We consider a two-dimensional problem. Here, the free energy functional F minimized by the phase field profile that generates a triangular lattice structure is given by [1, 2]

$$F = \int \left[\frac{\phi}{2} \left\{ \alpha + \lambda \left(q_0^2 + \nabla^2 \right)^2 \right\} \phi + \frac{u}{4} \phi^4 \right] dxdy , \tag{1}$$

where α is the driving force related to temperature. λ, q_0, and u are parameters unique to a given material. Also, the relation between a and q_0 is expressed by $\sqrt{3}/2 q_0 = 2\pi/a$. To obtain another atomic lattice structures, a different nonlinear term has to be chosen. For example, cubic symmetry can be obtained by replacing ϕ^4 with $|\nabla\phi|^4$ [8]. Since ϕ is the local time-averaged density and a conserved value, by following Chan-Hilliard equation, the time evolution equation for ϕ can be expressed as;

$$\frac{\partial \phi}{\partial t} = \nabla \cdot \left[\Gamma \nabla \frac{\delta F}{\delta \phi} \right] = \Gamma \nabla^2 \left[\left\{ \alpha + \lambda \left(q_0^2 + \nabla^2 \right)^2 \right\} \phi + u\phi^3 \right], \tag{2}$$

where Γ is the phase field mobility. Additionally, if we need thermal fluctuations, conserved Gaussian correlated noise fields are added to the right side of Eq. 2. For simplicity, however, the noise term is not considered in this study. Here, assuming $(a, \lambda, u) = (2\pi, 1, 1)$, the phase diagram can be derived from Eq. 1 as shown in Fig. 2(a).
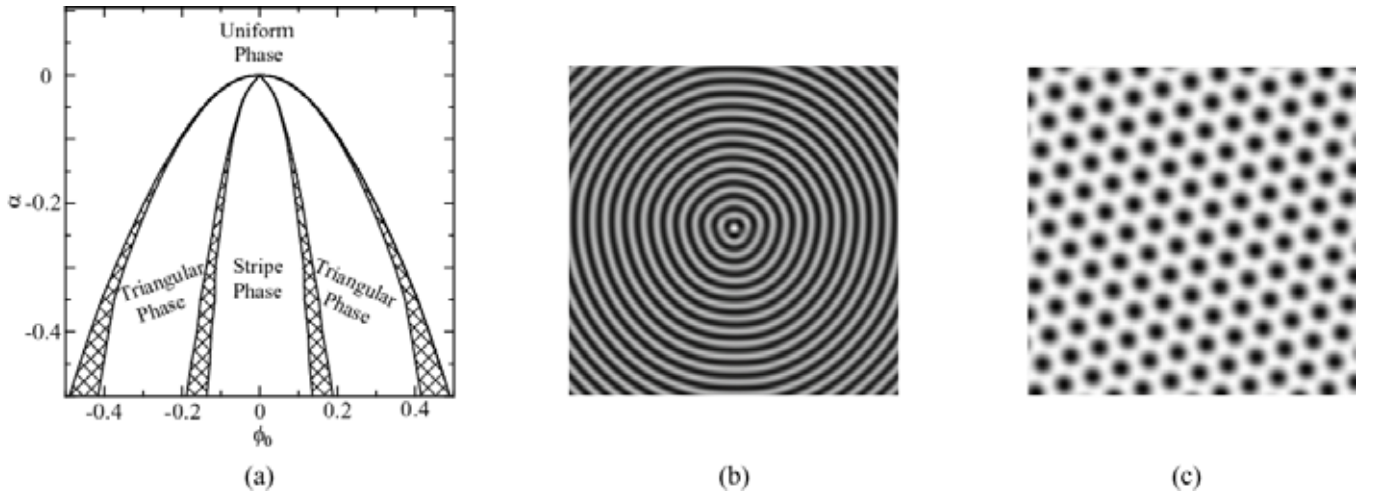

Fig. 2 (a) Phase diagram in two dimensions, (b) stripe phase and (c) triangular phase.

This diagram shows that the phase in the equilibrium state is determined by choosing α and ϕ_0. Figures 2 (b) and (c) show the typical stripe and triangular phases, respectively. Additionally the uniform phase corresponds to the liquid phase. The hatched areas in Fig. 2 (a) are the coexistence regions of stripe and triangular phases, or triangular and uniform phases.

NUMERICAL SIMULATIONS AND RESULTS

The deformation behavior of nanopolycrystalline structures with regular hexagonal grains is simulated by the PFC method two-dimensionally and investigated in detail. Before deformation simulation, regular hexagonal grain structures with predetermined orientations are prepared by solidification simulation.

1. Computational model for solidification Figures 3 (a) and (b) show the initial and boundary conditions and the desired grain structure, respectively.
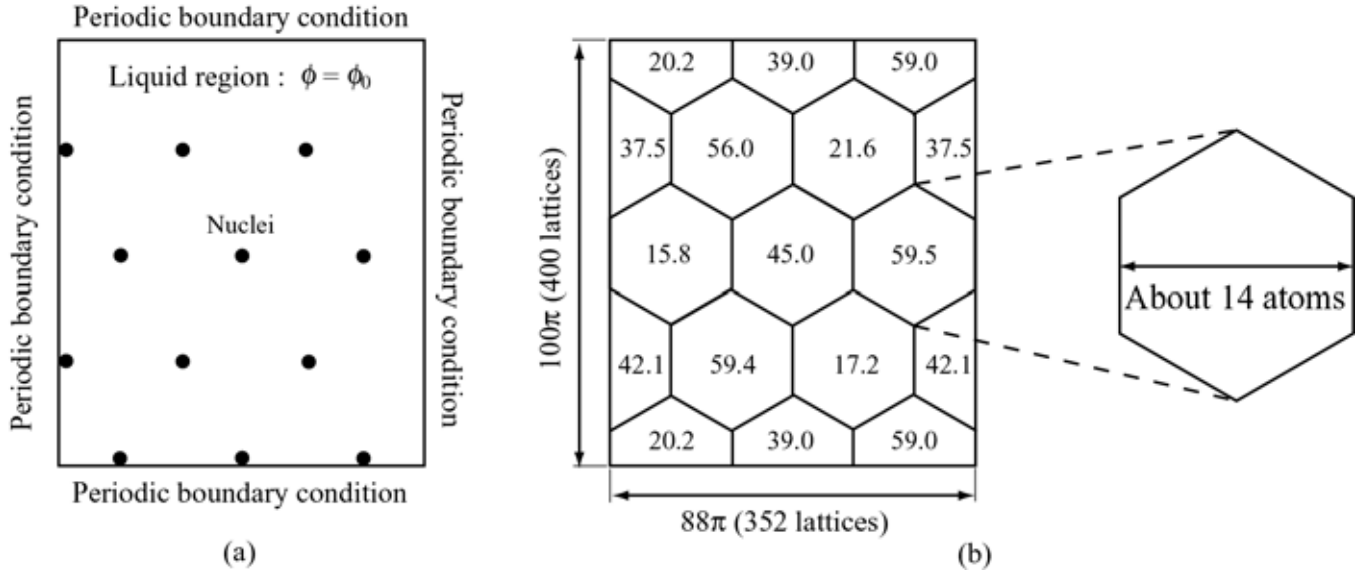

Fig. 3 Computational model for solidification. (a) Initial and boundary conditions and (b) desired grain structure.

Computation is performed on a rectangular domain of $100\pi \times 88\pi$ with uniform grids of $\Delta x = \Delta y = \pi/4$. The initial condition has twelve nuclei on the liquid phase in which ϕ is constant, $\phi_0 = -0.31$. As shown in Fig. 3 (a), nuclei are disposed at the center of the regular hexagonal grains shown in Fig. 3(b). There are about 14 atoms between the two sides of the hexagonal grain. Three crystal orientations, i.e., $\theta = 0, 20, 40$ degrees, are employed to form high-angle grain boundaries, and, using random variables, the orientations are made to deviate from the initial values. Periodic boundary conditions are adopted in all directions. The model parameters $(\alpha, \Gamma, \Delta t) = (-0.30, 1, 0.01)$ are selected in this simulation.

2. Results of solidification simulation Figure 4 shows the evolution of solidification microstructures. With time, crystalline phases grow and impinge, finally forming grain boundaries. The number of dislocations on each grain boundary differs depending on the misorientation between grains. From the orientations measured by solid lines drawn along the atomic arrangement in Fig. 4(c), it is confirmed that the predetermined orientations in Fig. 3(b) are achieved at the completion of solidification simulation. Figure 5 shows the time slices of the phase field in the square red area of Fig.4(c). In Figs. 5 (a) and (b), nuclei grow into a liquid phase. In Fig. 5(c), solid phases impinge on each other. In the collision domain, the phase field distribution loses periodicity. After the collision, the boundaries of the crystals become evident (Fig.5 (d)). The disorder regions become narrow with time (Fig. 5(e)). Finally, as shown in Fig. 5(f), sharp grain boundaries are formed.
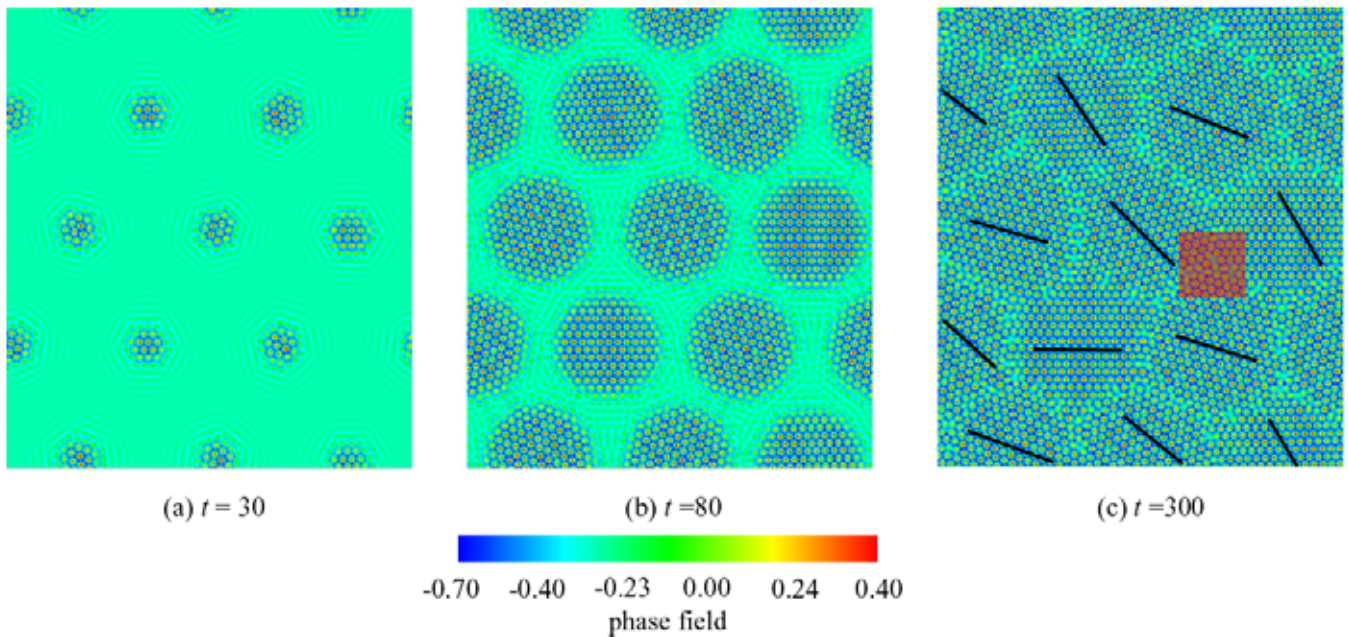
(a) $t = 30$ (b) $t = 80$ (c) $t = 300$

-0.70   -0.40   -0.23   0.00   0.24   0.40
phase field

Fig. 4 Evolution of solidification microstructure.

(a) $t = 30$ (b) $t = 80$ (c) $t = 100$

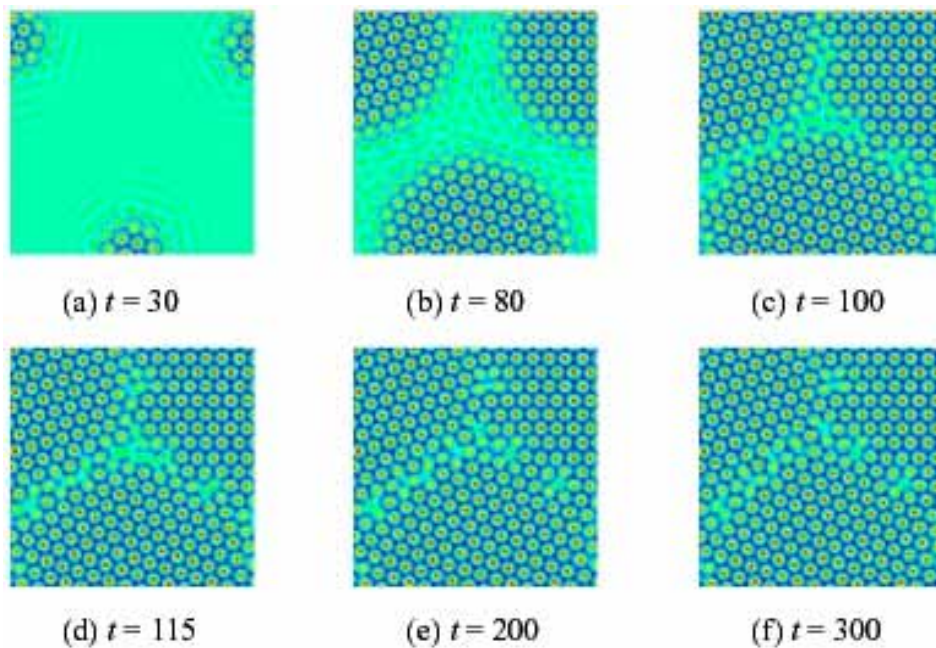(d) $t = 115$ (e) $t = 200$ (f) $t = 300$

Fig. 5 Phase field profiles of square region in Fig. 4(c).

3. Computational model for deformation Figure 6 shows a technique of applying tensile deformation to the nanopolycrystalline structures prepared by solidification simulation. Additional computational domains with a width of $40\Delta x$ are attached to the left and right ends of the prepared nanocrystalline structures. The phase field inside the additional domains is set to be $\phi = \phi_0$ that mean the liquid phase. The phase field profiles inside the "fixed area" are fixed during deformation simulation and the "fixed area" is moved with tensile deformation rate. Periodic boundary conditions are used at the top and bottom boundaries.
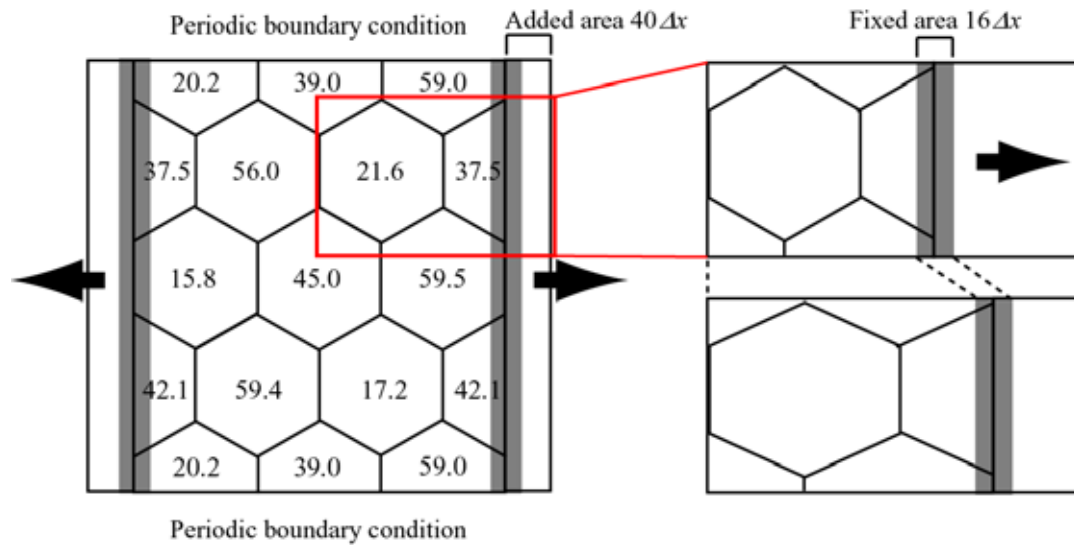
Fig. 6 Technique of tensile deformation.

4. Results of deformation simulation Figure 7 shows the phase field distributions at $\varepsilon = 0.000$, 0.063, and 0.130. In Fig. 7(b), the grain shapes change from the initial hexagonal shape shown in Fig. 7(a) with grain boundary migration and grain rotation. As strain increases, grain coalescence begins to occur. However, no dislocations in the grains are observed. As the reason for this, it is considered that the grain size is too small for dislocations to penetrate into the grain [7]. Therefore, it is clarified in this simulation that intergranular deformation is the predominant deformation mode. Next, we examine in detail the deformation behavior in the square region in Fig. 7(a), in which grain coalescence is prominent. Figure 8 shows close-up views of the square region in Fig. 7(a).
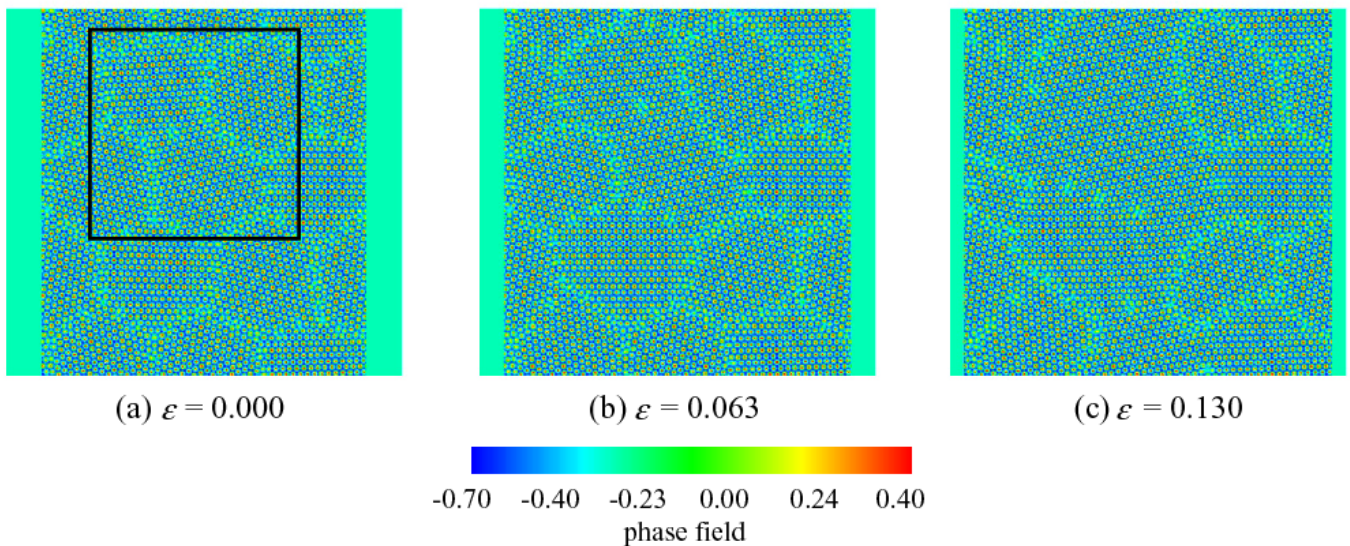

(a) $\varepsilon = 0.000$ (b) $\varepsilon = 0.063$ (c) $\varepsilon = 0.130$

-0.70   -0.40   -0.23   0.00   0.24   0.40
phase field

Fig. 7 Phase field distributions at $\varepsilon =$ (a) 0.000, (b) 0.063 and (c) 0.130.

The insets on the upper right corner of Figs. 8 (a) – (i) indicate the crystal orientations of grains A, B and C by segment lines. From Fig. 8(a), the initial misorientation between grains A and B is small, on the other hand, those between grains C and A and C and B are large. As strain increases (Fig. 8(b) – (c)), crystal grain

rotation begins to occur between grains A and B. Moreover, triple junctions shown by the open circle in Fig. 8(b) begin to move in order to maintain the balance in grain boundary energy. Therefore, the grain boundary between grains A and B migrates in response to the movement of the triple junctions. In Figs. 8(d) – (e), grains A and B continuously rotate so as to reduce their misorientation. Then, a dislocation surrounded by a square region quickly glides toward the grain boundary between grains A and E. As a result, the grain boundary between grains A and B disappears after the fusion of grains A and B. On the other hand, although grain C is adjacent to grains A and B, this grain shows no rotation. In Figs. 8(g) – (i), since the coalescence of grains A and B results in the elimination of the triple junctions shown in Fig. 8(b), grain boundary migration is accelerated due to the curvature of grain boundary. Thus, the coarsening of integrated grain A-B is caused by grain boundary migration.
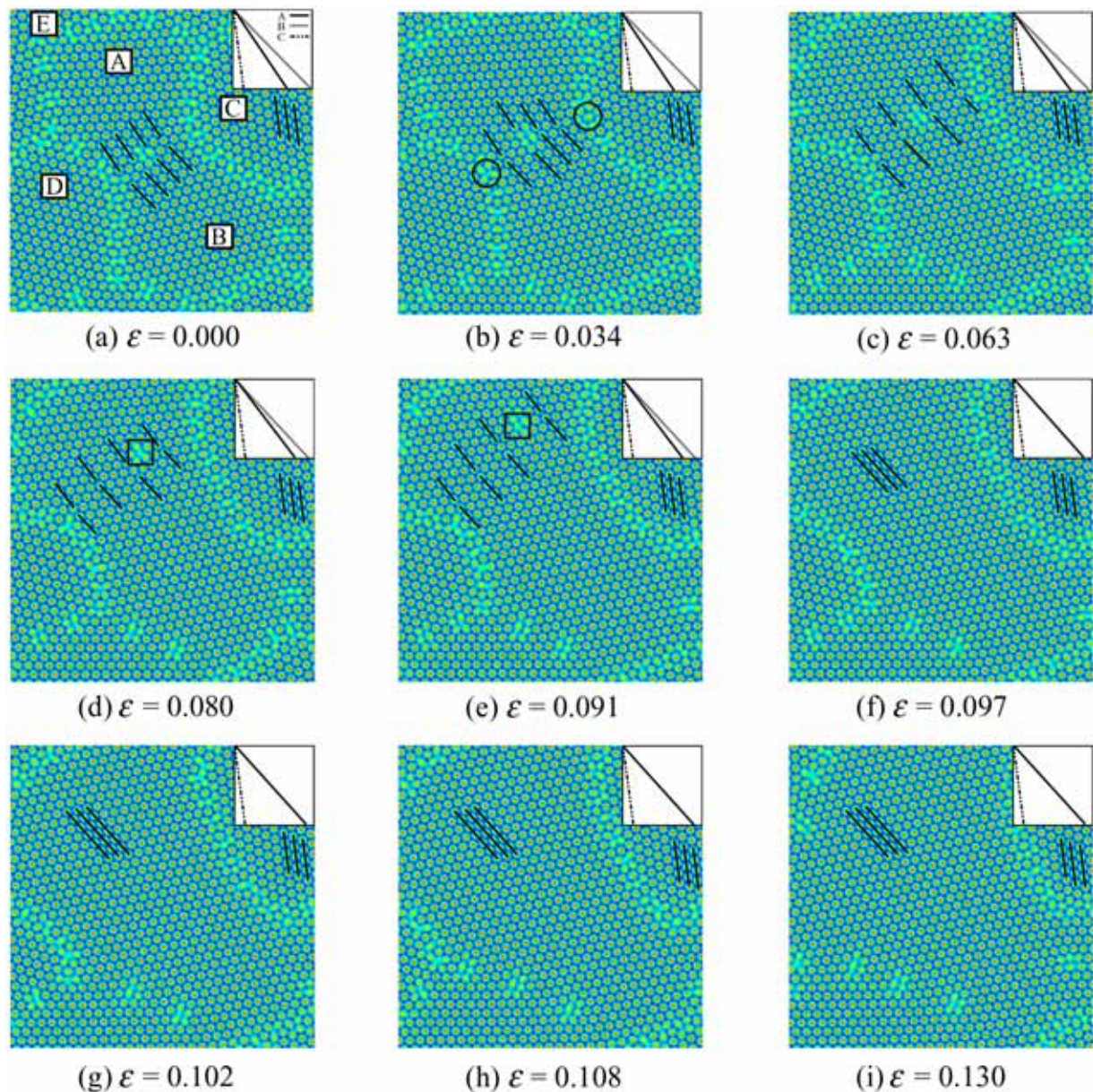

(a) $\varepsilon = 0.000$

(b) $\varepsilon = 0.034$

(c) $\varepsilon = 0.063$

(d) $\varepsilon = 0.080$

(e) $\varepsilon = 0.091$

(f) $\varepsilon = 0.097$

(g) $\varepsilon = 0.102$

(h) $\varepsilon = 0.108$

(i) $\varepsilon = 0.130$

Fig. 8 Deformation process shown in square region in Fig. 7(a).

CONCLUSIONS

The plastic deformation of nanopolycrystalline metals is studied using the phase field crystal method at a realistic strain rate of about 10^0 s^{-1}. Before deformation simulation, nanopolycrystalline structures with regular hexagonal grains are generated during solidification simulation. Here, the crystal orientations are controlled in order to achieve predefined orientations. In the deformation simulation, it is observed that intergranular deformation, that is, grain rotation and grain boundary migration, is the predominant deformation mechanism. Grain rotation occurs in two neighboring grains with small misorientations. The integrated grain caused by the rotation is further coarsened by the accelerated grain migration.

REFERENCES

[1] E. R. Elder, M. Katokowski, M. Haataja, M. Grant, *Modeling Elasticity in Crystal Growth*, Phys. Rev. Lett. **88**, (2002), 245701.

[2] E. R. Elder, M. Grant, *Modeling elastic and plastic deformations in nonequilibrium processing using phase field crystals*, Phys. Rev. E **88**, (2004), 051605.

[3] J. Berry, M. Grant, E. R. Elder, *Diffusive atomistic dynamics of edge dislocations in two dimensioins*, Phys. Rev. E **73**, (2006), 031609.

[4] M. A. Meyers, A. Mishra, D. J. Benson, *Mechanical properties of nanocrystalline materials*, Prog. Mater. Sci. **51**, (2006), 427-556.

[5] C. C. Koch, *Optimization of strength and ductility in nanocrystalline and ultrafine grained metals*, Scr. Mater. **49**, (2003), 657-662.

[6] J. Schiotz, K. W. Jacobsen, *A Maximum in the Strength of Nanocrystalline Copper*, Science **301**, (2003), 1357.

[7] T. Shimokawa, A. Nakatani, H. Kitagawa, *Grain-size dependence of the relationship between intergranular and intragranular deformation of nanocrystalline Al by molecular dynamics simulations*, Phys. Rev. B **71**, (2005), 224110.

[8] A. A. Golovin, A. A. Nepomnyashchy, *Disclinations in square and hexagonal patterns*, Phys. Rev. E **67**, (2003), 056202.